

Edith Cowan University
Research Online

ECU Publications Pre. 2011

1-1-2010

Adiabatic coherent quantum tunneling of ultracold atoms trapped in an asymmetrical two-dimensional magnetic lattices

Ahmed Abdelrahman
Edith Cowan University

Kamal Alameh
Edith Cowan University

Peter Hannford
Swinburne University of Technology

Follow this and additional works at: <https://ro.ecu.edu.au/ecuworks>

 Part of the [Engineering Commons](#)

[10.1109/HONET.2009.5423089](https://ro.ecu.edu.au/ecuworks/6466)

This is an Author's Accepted Manuscript of: Abdelrahman, A., Alameh, K., & Hannford, P. (2010). Adiabatic coherent quantum tunneling of ultracold atoms trapped in an asymmetrical two-dimensional magnetic lattices. Proceedings of High-Capacity Optical Networks and Enabling Technologies (HONET). (pp. 120-124). Alexandria, Egypt. IEEE Press. Available [here](#)

© 2010 IEEE. Personal use of this material is permitted. Permission from IEEE must be obtained for all other uses, in any current or future media, including reprinting/republishing this material for advertising or promotional purposes, creating new collective works, for resale or redistribution to servers or lists, or reuse of any copyrighted component of this work in other works.

This Conference Proceeding is posted at Research Online.
<https://ro.ecu.edu.au/ecuworks/6466>

Adiabatic Coherent Quantum Tunneling of Ultracold Atoms Trapped in an Asymmetrical Two-Dimensional Magnetic Lattices

A. Abdelrahman^{*†}, K. Alameh[†] and P. Hannaford[‡]

[†] *Electron Science Research Institute, Edith Cowan University
270 Joondalup Drive, Joondalup Perth, 6027 WA, AUSTRALIA*

[‡] *Center for Atom Optics and Ultrafast Spectroscopy,
and ARC Centre of Excellence for Quantum Atom Optics
Swinburne University of Technology, Melbourne, Australia 3122*

^{*} a.abdelrahman@ecu.edu.au

Abstract—We propose a new method to realize a two-dimensional magnetic lattice, having two different configurations of asymmetric magnetic lattice, which exhibits magnetic band gap structure, and a symmetric magnetic lattice. We also describe the tunneling mechanisms of magnetically trapped ultracold atoms, prepared in a degenerate quantum gas such as Bose-Einstein Condensate (BEC). A coherent quantum tunneling of ultracold atoms between the sites of the asymmetrical magnetic lattice can be realized which induces the adiabatically controlled *dc* Josephson current. At critical phase transitions, namely at certain values of site phase difference and population fraction, a plasma oscillation can be observed in which it forms a discharging Josephson state to be used as coherently coupled *n* quantum bits.

I. INTRODUCTION

The use of magnetic micro-traps to manipulate atoms in quantum degenerate gases, such as Bose-Einstein condensate and ultracold fermions, has attracted a considerable attention and interest in the area of condensed matter. Now magnetic micro-traps can be used to simulate condensed matter problems where recently several reports have pointed out the significant use of these quantum devices to this approach. They can be regarded as micro-potential wells similar to that in semiconductor devices where atoms play as spin particles, e.g., electrons and holes [1]. One of the interesting problems in condensed matter physics that widely investigated using trapped ultracold atoms is the Josephson physics at low temperature [1][2].

There are various approaches to magnetically trap ultracold atoms, such as current carrying wires and permanently magnetized material atomic traps [3], [4], [5], [6]. The method of trapping varies from optical trapping to magnetic trapping where ultracold atoms are arranged in one or two-dimensional lattice-like structure [7]. In such configurations and due to the tight confinement and the very low temperature of atoms, coherent control of several degrees of freedom of specific

quantum states can be achieved leading to interesting answers and observations for critical phase transitions.

We adopted the approach of a permanent magnet ultracold atoms trap where in this article we explain how to use our simple method to create the so called magnetic lattice with two different configurations. In section (II), we describe our approach of how to realize the asymmetrical magnetic lattice in which it creates several magnetic bands having different magnetic minima. In section (III), we explain the Bose-Hubbard model as a possible second-quantized to describe the field interaction of the trapped ultracold atoms., while in section (IV) we show the relevant parameters that are used to calculate the condition for the adiabatic flow of the *dc* Josephson current to be induced between the lattice sites. We conclude in section (V) by drawing possible applications of this approach.

II. TWO-DIMENSIONAL MAGNETIC LATTICE

The Magnetic lattice based quantum device is realized by milling an $m \times m$ array of blocks, each block being an array of $n \times n$ square holes of size α_h , separated by α_s , where n represents the number of holes in a block as detailed in Figures 1(a)-1(b). The gaps between the blocks containing no holes are assumed to be greater than, or equal in width to α_s . The holes are formed, within a magneto-optic thin film of thickness τ_{btm} sputtered onto a proper substrate. The depths of all holes are equal and extend through the thin film thickness down to the substrate surface level. The gaps separating different blocks are an important design feature which enables the $n \times n$ magnetic lattices to be surrounded by an unperturbed film area, which introduces an extra degree of confinement through the creation of magnetic field "walls" encircling the $n \times n$ matrices, and isolating them from one another. The magnetic quantum device is in its remanently-magnetized state, where its magnetization direction is perpendicular to the surface

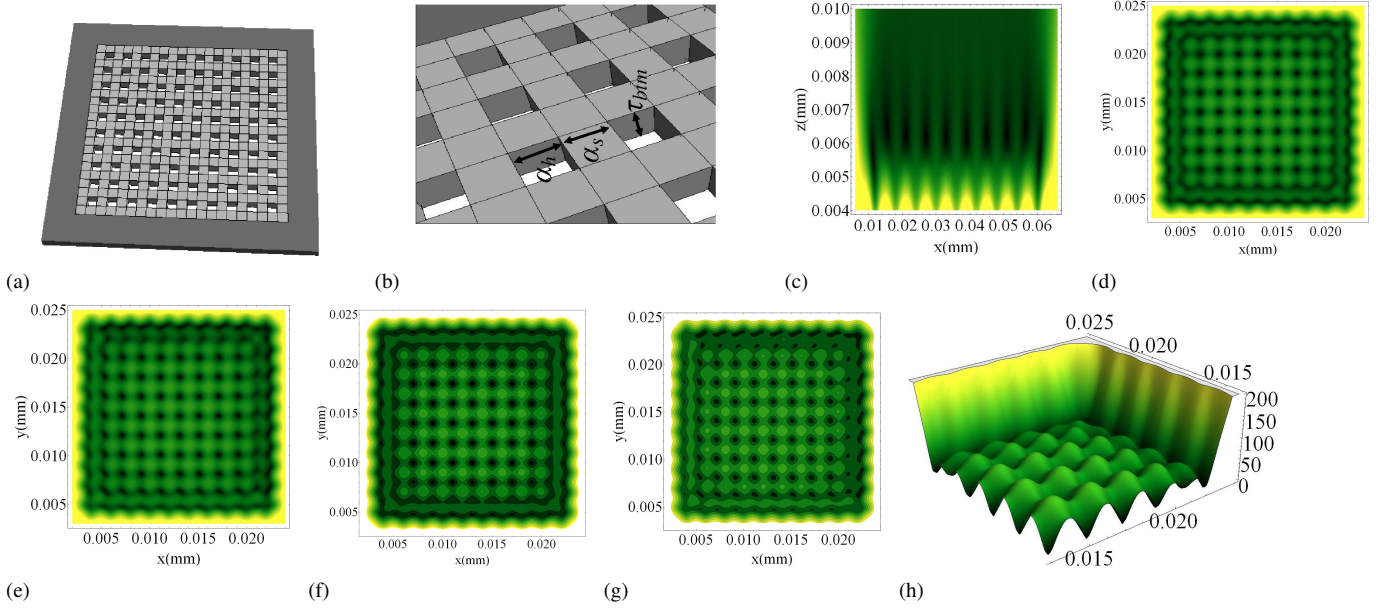


Fig. 1. (a) A 10×10 magnetic lattice surrounded by an unperturbed area. (b) The lattice parameters are specified by the hole size $\alpha_h \times \alpha_h$, the periodic spacing α_s between the holes and the magnetic layer thickness τ_{btm} . (c) Magnetic density plot of the simulated magnetic lattice sites at $z - x$ plane along the center of the lattice. The traps (dark color) are located at the effective z -distance, d_{min} , from the holes opening centers of high magnetic field (bright color) above the film plane. (d-e) Magnetic field density plot across the $x - y$ plane at the d_{min} with no external magnetic bias fields and with application of the external $B_{x-bias} = 10G$ and $B_{y-bias} = 10G$ magnetic bias fields, respectively. (f-g) Contour plot of distributed lattice sites across the $x - y$ plane without and with applications of $B_{x-bias} = 10G$ and $B_{y-bias} = 10G$ respectively. (h) 3D plot of the magnetic field (on the z -axis) of the distributed sites across the $x - y$ plane (x -axis and y -axis) simulated at the d_{min} and displayed from the center sites to the edge sites where $B_{x-bias} = 10G$ and $B_{y-bias} = 10G$ were applied. Simulation input: $\alpha_s = \alpha_h = 1\mu m$, $M_z = 3kG$, $\tau_{btm} = 2\mu m$ and $\tau_{p-wall} = 1\mu m$.

plane. Effective parameters of the magnetic lattice for small values of n are considered, however some cases for large n are presented.

The structure generates two dimensional periodically distributed magnetic field minima in the vicinity of the surface of the perforated film where the distribution creates the magnetic lattice that used to trap the cold atoms. The presence of holes results in a magnetic field distribution whose non-zero local minima are located at effective z -distances from the holes opening centers above the film plane. These minima are localized in small volumes representing the potential wells that contain certain number of quantized energy levels for the cold atoms to occupy. In our design, we assumed that the size of the holes α_h and the holes separation α_s are both equal, $\alpha_h = \alpha_s \equiv \alpha$, to simplify the mathematical derivation where we adopted an analysis approach similar to that reported in [4], [8]. The spatial magnetic field components B_x , B_y and B_z can be written analytically as a combination of a field decaying away from the surface of the trap in the z -direction and a periodically distributed magnetic field in the $x - y$ plane produced only by the magnetic induction, B_o , at the surface of the permanently magnetized thin film, where $B_o = \mu_o M_z / \pi$. We define the surface reference magnetic field as $B_{ref} = B_o(1 - e^{-\beta\tau})$, where $\beta = \pi/\alpha$, $\tau = \tau_{btm}$ is the film thickness, and the plane of symmetry is assumed at $z = 0$. Figure 1(d-g) show the simulated map of the magnetic field strength distribution across the $x - y$ planes located at different distances above the magnetized film surface. Both the

density plot and contour plot representation types are shown for both simulation results of a 10×10 magnetic lattice at the initial magnetic state, formed by B_{ref} only, and with the external application of B_{x-bias} and B_{y-bias} , respectively. The analytical expressions that describe the non-zero local minima, periodically positioned in the $x - y$ plan, take into account the strength of the effective field and α [8]. These expression are derived and simplified to the following set of equations

$$B_x = B_o \left(1 - e^{-\beta\tau}\right) e^{-\beta[z-\tau]} \sin(\beta x) - \frac{B_o}{3} \left(1 - e^{-3\beta\tau}\right) \times e^{-3\beta[z-\tau]} \sin(3\beta x) + \dots + B_{x-bias} \quad (1)$$

$$B_y = B_o \left(1 - e^{-\beta\tau}\right) e^{-\beta[z-\tau]} \sin(\beta y) - \frac{B_o}{3} \left(1 - e^{-3\beta\tau}\right) \times e^{-3\beta[z-\tau]} \sin(3\beta y) + \dots + B_{y-bias} \quad (2)$$

The component of the magnetic field along the z -axis, B_z , is given by

$$B_z = B_o \left(1 - e^{-\beta\tau}\right) e^{-\beta[z-\tau]} \left[\cos(\beta x) + \cos(\beta y) \right] - \frac{B_o}{3} \left(1 - e^{-3\beta\tau}\right) e^{-3\beta[z-\tau]} \left[\cos(3\beta x) + \cos(3\beta y) \right] + \dots + B_{z-bias} \quad (3)$$

The higher order terms in these equations can be neglected for distances that are large compared to the effective distance. This is because only the cold atoms that are in the so called *low*

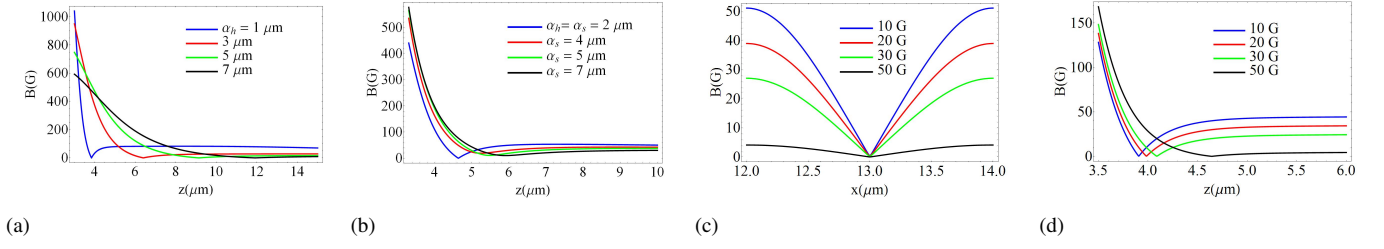


Fig. 2. (a) The effect of changing the size of the holes, α_h , on the location of the magnetic field local minima along the z -axis, B_{min}^z located at d_{min} above the hole opening center at the surface of the thin film, and (b) the effect of changing the periodicity length, α_s , across the $x - y$ plane. (c) Simulation result of varying the tunneling barrier heights ΔB_x through change in the z -axis magnetization, M_z by applying external B_{z-bias} magnetic field in the negative z -direction, and (d) B_{z-bias} effect on the gradient of the magnetic sites near the local minima along the z -axis. The thin film thickness: $\tau_{btm} = 2 \mu m$ is used in all cases.

magnetic field seeking – state (atom's magnetic moment to be oriented antiparallel to the localized magnetic field in the trap) are attracted to the non-zero local minima of the magnetic traps located at the effective z -distance from the film surface, which is larger than $\alpha/2\pi$. Thus, Equations (1) to (3) can now be simplified as

$$B_x = B_o \left(1 - e^{-\beta\tau}\right) e^{-\beta[z-\tau]} \times \sin(\beta x) + B_{x-bias} \quad (4)$$

$$B_y = B_o \left(1 - e^{-\beta\tau}\right) e^{-\beta[z-\tau]} \times \sin(\beta y) + B_{y-bias} \quad (5)$$

$$B_z = B_o \left(1 - e^{-\beta\tau}\right) e^{-\beta[z-\tau]} \times \left[\cos(\beta x) + \cos(\beta y)\right] + B_{z-bias} \quad (6)$$

The magnitude \mathbf{B} of the magnetic field above the film surface can be written, using Equations (4) to (6), as

$$\mathbf{B} = \left\{ B_{x-bias}^2 + B_{y-bias}^2 + B_{z-bias}^2 + 2B_o^2 \left(1 - e^{-\beta\tau}\right)^2 e^{-2\beta[z-\tau]} \left[\cos(\beta x)\cos(\beta y)\right] + 2B_o^2 \left(1 - e^{-\beta\tau}\right) e^{-\beta[z-\tau]} \left(\left[B_{x-bias} + B_{z-bias} \right] \cos(\beta x) + \left[B_{y-bias} + B_{z-bias} \right] \cos(\beta y) \right) \right\}^{1/2} \quad (7)$$

The simulation result of numerical calculations for a finite magnetic lattice are shown in Figure 3 which shows the location of the magnetic field non-zero local minima, B_{min}^z , along the z -axis at the effective distance, d_{min} , from the hole opening center and confined along z -axis by a magnetic barrier of magnitude ΔB_z . The results shown in Figure 3(b) demonstrate the existence of non-zero local minima of the magnetic field at the effective z -distance along the x -axis, confirming the suitability of the structure proposed for trapping cold atoms prepared in the low magnetic field seeking state.

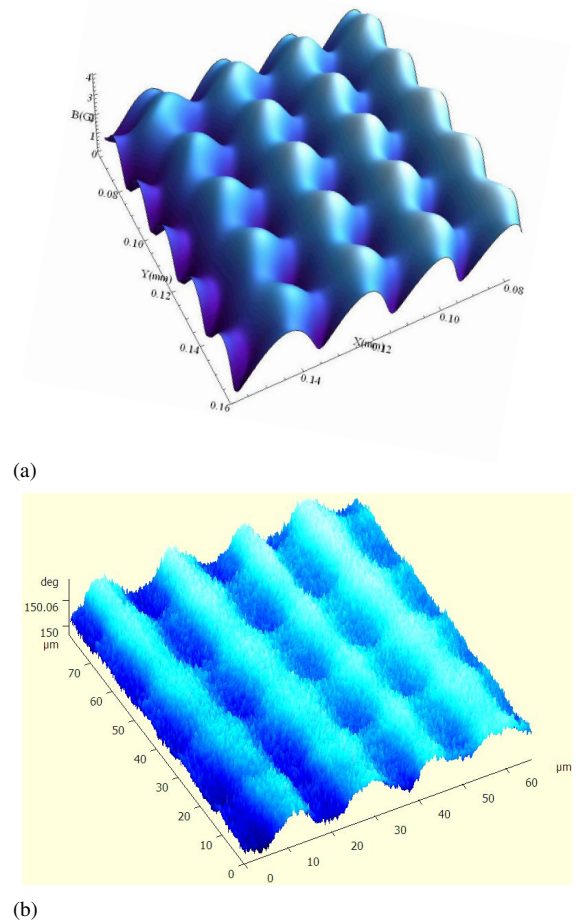


Fig. 3. (a) The magnetic field minima B_{min}^z simulated across the surface of the magnetic lattice, where we simulate the application of bias field along x -axis, $B_{x-bias} = 2$ G. (b) Magnetic Force Microscope (MFM) measurement showing the phase across the surface with the same conditions applied in simulation. Simulation input of the magnetic lattice characteristic parameters: $M_z = 3$ kG and $\tau_{btm} = 1 \mu m$.

III. DISCRETE MULTI-QUANTUM STATES IN THE ASYMMETRICAL MAGNETIC LATTICE

The asymmetric behavior in the proposed magnetic lattice, which is created due to the existence of different levels of the non-zero magnetic local minima, exhibits different magnetic bands separated by a gap of tilting potential δB . We denote such effect as magnetic band gap structure, similar to semiconductor devices. The magnetic band gap structure in our lattice contains several bands regarded as several conduction and valence bands. Each band described by its magnetic minima distributed across the $x - y$ plane. These minima are the magnetic lattice sites having a tight magnetic field confinement. Due to this confinement there are several on-site quantum energy levels available allowing the two-state characteristic to be applied at each site where we ignore in our approximation the higher energy levels of the site [9]. We describe our system considering the two-level quantum system configuration in which at each individual site, at the i th magnetic band, there is the vibrational ground state ϕ_i^g and vibrational excited state ϕ_i^e , where $i \in \{1, 2, \dots, n\}$ is the potential well index starting from the center site. These two modes are in a linear superposition when tunneling, and hence the interaction, between two adjacent bands. Such superposition describes the many Schrödinger cat-state which can be written, for simplicity, as a one-directional transitions

$$\Psi = \sum_{i=1}^{n-1} \phi_i^g + \phi_{i+1}^e \quad (8)$$

Where the coupling is between the i th site ground state and the $(i + 1)$ th excited state. The one-directional transition can be generalized to describe the superposition of all sites in the two-dimensional magnetic lattice.

• The Model

We consider the two lowest energy states, ϕ_i^g and ϕ_i^e , in each individual potential well, are closely spaced and sufficiently separated from the other higher levels within the well, permitting the two-mode approximation of the many-body problem in our proposed magnetic lattice [10]. The Bose-Hubbard model describes the bosons-bosons interaction of the on-site, or the self-trapped ultracold atoms, and intra-site tunneling process [11]. This general second-quantized Hamiltonian, in terms of bosonic creation, $\hat{\Phi}^\dagger(\mathbf{x})$, and annihilation, $\hat{\Phi}(\mathbf{x})$, field operators, for a system of N interacting boson of mass M confined by the external conservative time varying magnetic potential $B(\mathbf{x}, t)$ at zero temperature is given by

$$\begin{aligned} \hat{H} = & \sum_{i \neq j} \int d^3 \mathbf{x} \hat{\Phi}_i^\dagger(\mathbf{x}) \left[-\frac{\hbar^2}{2M} \nabla^2 + \mathbf{B}(\mathbf{x}, t) \right] \hat{\Phi}_i(\mathbf{x}) + \\ & + \sum_i^n \int d^3 \mathbf{x} d^3 \hat{\mathbf{x}} \hat{\Phi}_i^\dagger(\mathbf{x}) \hat{\Phi}_{i+1}^\dagger(\hat{\mathbf{x}}) U_{i,i+1}(\mathbf{x}, \hat{\mathbf{x}}) \hat{\Phi}_{i+1}(\hat{\mathbf{x}}) \hat{\Phi}_i(\mathbf{x}) \end{aligned} \quad (9)$$

where

$$\hat{\Phi}(\mathbf{x}) = \sum_{i=1}^n \hat{a}_i \phi_i(\mathbf{x}), \quad \hat{\Phi}^\dagger(\mathbf{x}) = \sum_{i=1}^n \hat{a}_i^\dagger \phi_i^*(\mathbf{x}) \quad (10)$$

The cold atoms tunnel, through a quantum cold collision process, within the usual s -wave scattering length, a_s , described by the interaction potential $U_{i,i+1}(\mathbf{x}, \hat{\mathbf{x}})$ in the second term of the above Hamiltonian, equation (9), such that

$$\begin{aligned} U_{i,i+1}(\mathbf{x}, \hat{\mathbf{x}}) = & g \int d\mathbf{x} |\phi_i^g(\mathbf{x})|^2 |\phi_{i+1}^e(\hat{\mathbf{x}})|^2 \\ & \rightarrow \frac{4\pi\hbar^2 a_s^{i,i+1}}{M} \delta^4(\mathbf{x} - \hat{\mathbf{x}}) \end{aligned} \quad (11)$$

which reduces to be equal to the coupling strength, g , between the two states ϕ_i^g and ϕ_{i+1}^e , in the s -wave scattering range. When tunneling is allowed, the coupling between the two modes is described by rewriting the Bose-Hubbard model (9) in terms of the hopping strength(tunneling) $J_{i,i+1}(\mathbf{x}, \hat{\mathbf{x}})$ between the adjacent magnetic bands where the tunneling of the ultracold atoms between sites is also affected by the tilting magnetic field δB . Introducing the number operator $\hat{n}_i = \hat{a}_i^\dagger \hat{a}_i$, one can write the above Hamiltonian in equation (9) as

$$\begin{aligned} \hat{H}' = & \sum_{i \neq j} J_{i,j} (\hat{n}_i - \hat{n}_j) + \sum_{i \neq j} \frac{U_{ij}}{N} (\hat{n}_i [\hat{n}_i - 1] + \\ & + \hat{n}_j [\hat{n}_j - 1]) + \delta B \sum_{i \neq j} (\hat{a}_i^\dagger \hat{a}_j + \hat{a}_j^\dagger \hat{a}_i) \end{aligned} \quad (12)$$

where \hat{a}^\dagger and \hat{a} obey the usual commutation relations, and the tunneling parameter $J_{i,i+1}$ defined as

$$J_{i,i+1}(\mathbf{x}, \hat{\mathbf{x}}) = \int d\mathbf{x} \phi_{i,i+1}^*(\mathbf{x} - \hat{\mathbf{x}}) \left[\frac{\hbar^2}{2M} \nabla^2 + \mathbf{B}(\mathbf{x}, t) \right] \phi_{i,i+1}(\mathbf{x} - \hat{\mathbf{x}}) \quad (13)$$

Using the Hamiltonian (12), we can describe two well known regimes formed in this type of magnetic lattices, [12]. In case of self-trapping, where the condition $U_{i,i+1} \gg J_{i,i+1}$ holds, the ground state ϕ_i^g of each site is assumed to be equally occupied by certain number of cold atoms or single atom. This is a maximal entanglement situation where the no-tunneling condition prepares the asymmetric magnetic lattice to host a $n \times n$ qubits. The self-trapping regime in the lattice can be addressed by the Fock regime where its ground state is the Mott insulator state.

The tunneling is allowed when the condition $U_{i,i+1} \ll J_{i,i+1}$ holds. In case of magnetic lattice the scenario is similar to the optical lattices where the hopping strength $J_{i,i+1}$ is adiabatically controlled via the application of the external bias fields such as B_{z-bias} applied along the negative direction of z -axis. It is known as the Josephson regime because the tunneling of cold atoms between sites simulates the induced Josephson current (i.e., both ac and dc can be simulated) with adiabatically controlled flow as will be explained in the following section.

IV. ADIABATICALLY OSCILLATING JOSEPHSON DISCHARGING STATES

To simulate the physics of Josephson junctions we regard an n -weakly coupled macroscopic wave functions of n lattice

sites separated by a magnetic potential barrier ΔB , where the magnetic barrier height is given by [9]

$$\Delta B^i = B_{max}^i - B_{min}^i = \frac{\alpha_s^2}{2} \quad (14)$$

the holes separation is estimated to be $\alpha_s = \frac{\hbar^2}{M\kappa}$, in which κ is a function of the trap frequency ω_t , i.e., $\kappa = \hbar/2M\omega_t$. The local mode states, $\varphi_i(\mathbf{x}, t)$, are Gaussian and hence enables solving the self-consistent nonlinear Schrödinger equation or the Gross-Pitaevskii equation (GPE) [13]. The transition from self-trapping to Josephson oscillation is described by the GPE which can be written as

$$i\hbar \frac{\partial \varphi_i(\mathbf{x}, t)}{\partial t} = \left[-\frac{\hbar^2}{2M} \nabla^2 + \mathbf{B}(\mathbf{x}, t) + g \|\varphi_i(\mathbf{x}, t)\|^2 \right] \varphi_i(\mathbf{x}, t) \quad (15)$$

The process is purely a weakly interacting system in the s -wave scattering range governed by the inter-atomic scattering pseudo potential $g = \frac{4\pi\hbar^2 a_s}{M}$ of scattering length a_s . The set of n equations in (15), represent the nonlinear generalization of the sinusoidal Josephson oscillations occurring in superconducting junctions [2]. The Gaussian state have uniform amplitudes such that $\varphi_i(\mathbf{x}, t) = \sqrt{N_i} e^{i\theta_i}$, where N_i and θ_i are the number of cold atoms and the phase in each individual lattice site, respectively.

Introducing the phase difference $\zeta_i = \theta_i - \theta_{i+1}$ and the fractional population $-1 < \gamma = \sum_i^n (N_i - N_{i+1})/N < 1$, where N is the total number of cold atoms, we can write, following [2], the n Gross-Pitaevskii equation in terms of the ζ and γ as

$$\dot{\gamma}(\mathbf{B}, t) = -\sqrt{1 - \gamma^2} \sin(\zeta(\mathbf{B}, t)) \quad (16)$$

$$\dot{\zeta}(\mathbf{B}, t) = \chi\gamma + \frac{\gamma(\mathbf{B}, t)}{\sqrt{1 - \gamma^2(\mathbf{B}, t)}} \cos(\zeta(\mathbf{B}, t)) + \left[J_1 - J_{i+1} \right] \quad (17)$$

where $\chi = N^2 U/4K$, with U defined as in equation (11) and K defined as

$$K = - \int d\mathbf{x} \left[\frac{\hbar^2}{2M} \prod_{i=1}^n \nabla \phi_i + \mathbf{B}(\mathbf{x}, t) \prod_{i=1}^n \phi_i \right] \quad (18)$$

The above set of equations (16-17) represent the nonlinear generalization of the sinusoidal Josephson oscillations in the n site of the asymmetric magnetic lattice which is similar to that occurring in superconducting junctions. Simple mechanical analogue can be mapped to describe the system as a non-rigid pendulum. Based on this fact, at critical phase difference and fractional population the system undergoes the Josephson oscillation between the self-trapping and Josephson discharging state, where the discharging current represented as superconducting state induced by the tunneled cold atoms in which known as plasma oscillations and experimentally realized [14]. An interesting different dynamical phenomenon arises if the initial population imbalance is not equal to the critical value, to be reported elsewhere.

By setting (fabricating) the relevant value of α_s , one can induce the dc Josephson current adiabatically between the lattice site by applying the $B_{-z-bias}$. Ultracold atoms tunnel between sites starting from the center of the magnetic lattice to the edges due to the variation of the magnetic values of B_{min} between magnetic bands. Higher values of B_{min} exist at the center.

V. CONCLUSION

We have developed a new method to create two-dimensional magnetic lattice of symmetrically distributed lattice sites with equally spaced magnetic tunneling barriers across the $x - y$ plane. We have also shown that asymmetric distribution of the lattice sites, formed when only using the self reference magnetic field is possible. We have described a general scenario of the time evolution adiabatically controlled tunnel in which the tunneling process derives a slow dc Josephson current. The Josephson discharge oscillating states can handle a quantum register operations, where tunneling is used to transfer the qubits between the magnetic lattice sites. In addition we have shown that it is also possible to entangle a large number of lattice sites by preparing the trapped ultracold atoms in the Fock regime in which tunneling is not allowed and sites are assumed to have the critical phase difference and population fraction.

Our approach has shown that this method can simplify the difficulties in creating two dimensional magnetic lattice, where a large number of sites can be created and be equally distributed in a symmetrical configurations, to be reported elsewhere.

VI. ACKNOWLEDGE

We would like to thank James Wang, in Swinburne University in Melbourne, for his help in measuring the surface magnetic field using the Magnetic Force Microscope.

REFERENCES

- [1] S. Ashhab and C. Lobo, *Phys. Rev. B*, vol. 78, p. 041302, 2008.
- [2] A. Smerzi, S. Fantoni, S. Giovanazzi, and S. R. Shenoy, *Phys. Rev. Lett.*, vol. 79, p. 4950, 1997.
- [3] M. Singh, M. Volk, A. Akulshin, A. Sidorov, R. McLean, and P. Hannaford, *J. Phys. B: At. Mol. Opt. Phys.*, vol. 41, p. 065301, 2008.
- [4] S. Ghanbari, T. D. Kieu, A. Sidorov, and P. Hannaford, *J. Phys. B: At. Mol. Opt. Phys.*, vol. 39, p. 847, 2006.
- [5] B. V. Hall, S. Whitlock, F. Scharnberg, P. Hannaford, and A. Sidorov, *J. Phys. B: At. Mol. Opt. Phys.*, vol. 39, p. 27, 2007.
- [6] RADIA, <http://www.esrf.eu/>, vol. Version 4.1, 2009.
- [7] M. Singh, M. Volk, A. Akulshin, A. Sidorov, R. McLean, and P. Hannaford, *J. Phys. B: At. Mol. Opt. Phys.*, vol. 41, p. 065301, 2008.
- [8] S. Ghanbari, T. D. Kieu, A. Sidorov, and P. Hannaford, *J. Phys. B: At. Mol. Opt. Phys.*, vol. 40, p. 1283, 2007.
- [9] G. J. Milburn and J. Corney, *Phys. Rev. Lett.*, vol. 55, p. 4318, 1997.
- [10] Y. Shin, G.-B. Jo, M. Saba, T. A. Pasquini, W. Ketterle, and D. E. Pritchard, *Phys. Rev. Lett.*, vol. 95, p. 170402, 2005.
- [11] J. Javanainen, *Phys. Rev. Lett.*, vol. 57, p. 3164, 1986.
- [12] B. J. Dalton, *J. Mod Opt.*, vol. 54, p. 615, 2007.
- [13] A. P. Tonel, J. Links, and A. Foerster, *J. Phys. A: Math. Gen.*, vol. 38, p. 1, 2005.
- [14] M. Albiez, R. Gati, J. Fölling, S. Hunsmann, M. Cristiani, and M. K. Oberthaler, *Phys. Rev. Lett.*, vol. 95, p. 010402, 2005.